ISSN 1330-3651 (Print), ISSN 1848-6339 (Online)
https://doi.org/10.17559/TV-20230120000249
Original scientific paper

Finite Element Analysis of a Shrink Fitted Disc-Shaft Rotating System

Marko KATINIĆ*, Domagoj TRAVICA, Pejo KONJATIĆ, Mladen BOŠNJAKOVIĆ

Abstract: In this paper, the shrink fit between the conical disk and the rotor shaft of a steam turbine was analysed with the aim of determining the rotor speed at which this fit is lost. The analysis was carried out numerically using the finite element method (FEM) in the Ansys software package. Three design values of disc-shaft joint interference were considered: minimum, maximum and mean. The rotor speed at which the shrink fit is lost is the lowest for minimum interference and the highest for maximum interference, which was expected. In other words, the rotor speed at which the shrink fit is lost is a linear function of the amount of interference (the allowance). The results of the analysis showed that the considered interferences of the shrink fit ensured the smooth transmission of torque in the range of speeds up to the operating speed and that the operation of the turbine is safe from that point of view.

Keywords: conical disc; contact problem; finite element analysis; shaft; shrink fit

1 INTRODUCTION

Shrink fits are widely used to join mechanical parts. Shrink fit is a fastening of two tight fitting parts by pushing them together. The tightness of the fit is determined by the amount of interference of the fitted parts.

The application of shrink fits is particularly common in high-speed rotating machines. A typical example of a shrink fit is the connection between the bladed disc and the rotor shaft of a steam turbine. The shrink fit is achieved by mounting the cylindrical hub of the disc on the shaft, whereby the outer diameter of the shaft is greater than the inner diameter of the hub. There are two basic methods for fitting an oversized shaft into an undersized bore of the disc hub: force and thermal expansion [1]. Which method will be applied depends on the desired amount of interference. Contact interfacial pressure is generated due to interference and is the result of local elastic deformation. There is an expression [2] for calculating the contact pressure. A higher amount of interference results in a higher contact pressure and vice versa. Shrink fit disc-shaft should enable the transfer of torque during machine operation and should be safe for the entire lifetime of the machine rotor. The interference of the disc-shaft joint is reduced with increasing rotor running speed because of centrifugal force. Lack of interference in the disc-shaft joint is undesirable, as it can result in torque not being transmitted and cause vibration. This means that the interference must not be lower than the minimum value that ensures that the joint will not open up under operating conditions due to the lack of interference. This condition ensures that there is no slippage in the joint [1]. On the other hand, the interference must not be greater than the maximum value at which the disk and shaft can withstand the stresses generated during assembly and under the operating conditions of the machine. Therefore, the interference in the disc-shaft joint should be between minimum and maximum values.

Minimum interference condition would overcome differential radial growth between shaft and disc hub due to centrifugal loading and slip due to torsional loading during operation [1]. So, there is a rotor speed at which the interference would be lost, but for the minimum value of the interference, this rotor speed would be higher than the maximum operating speed of the machine. The rotor speed at which the interference would disappear can be determined by numerical calculation using FEM. At this speed, the contact pressure of the disc-shaft connection is reduced to zero.

Many of the previous papers deal with stress and strain analysis in stationary and rotating shrink fits [3-7]. There is a small number of researches on disc-shaft connection of steam turbine rotors [8, 9]. When designing a shrink fitted joint that rotates at a certain speed, analytical analysis is usually used to determine the minimum and maximum interference conditions. However, the analytical approach has a set of different limitations [8]. FEM analysis of the shrink fit provides additional information on the behaviour of the joint and its integrity.

In this paper, the rotor speed at which the interference between the conical bladed disc and the turbine rotor shaft disappears is considered. This speed is determined by numerical analysis for the minimum, maximum and mean design value of the interference. Numerical analysis was performed using Ansys software package [10]. Shrink fit is a typical example of a contact problem in which parts are held together by the action of frictional forces. As is already known, contact problems are highly non-linear and require significant computer capacities for solution [10]. A poorly defined contact in the Ansys software can lead to unstable conditions that usually mean poor convergence and wasted time. A well-defined contact will provide faster convergence and smoother results. In this paper, special attention was paid to the mesh quality and the setting of the contact formulation, which ensured a good convergence of the results.

2 FINITE ELEMENT ANALYSIS OF THE SHRINK FIT

Nowadays, most engineering tasks using numerical analysis are solved with satisfactory results using linear numerical approximation, that is, by applying the basic equation of the finite element method [11-18]. Given that nonlinear problems are more complex and cannot be described by the basic equation of the finite element method, it is necessary to define a nonlinear relation that is given by the expression [11]:

$$\boldsymbol{K}\left(\boldsymbol{V},\boldsymbol{R}\right)\boldsymbol{V}=\boldsymbol{R} \tag{1}$$

In the equation above, it can be seen that the stiffness matrix $\boldsymbol{K}$ is a function of the current state of displacement $\boldsymbol{V}$ and load $\boldsymbol{R}$. Furthermore, because of the nonlinear response, the problem cannot be solved in one step, so an iterative procedure is used until the convergence of the results is achieved. The convergence of the results is extremely important because it represents the reliability of the obtained numerical analysis results.

In numerical analysis, there are two basic types of contacts, linear and non-linear contacts. The main difference between the two types of contacts is the ability to move in a direction perpendicular to the contact surface.

The type of contact used in the analysis of the shrink fit is "Frictional Contact", shown in Fig. 1. This type enables the friction factor to be defined, in order to simulate the actual behavior of the shrink fit as realistically as possible. A value of 0,15 was chosen for the value of the friction factor during the verification of the shrink fit (the value of the friction factor between the steel - steel surface ranges from 0,07 to 0,16) [11]. The friction factor primarily depends on the material and the roughness of the surfaces in contact.

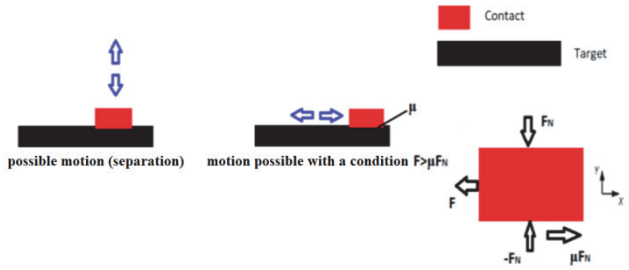

Figure 1 Definition of frictional contact [12]

Contact problems in the case of a shrink fit can best be described by the "Augmented Lagrange" method, which is a newer and improved version of the "Penalty Method". The "Penalty Method" formulation is based on the surface pressure between the contact surfaces, and penetration can be determined using the load and surface stiffness. The basic formulation is given by the expression [12]:

$$F_{\mathrm{N}} = k_{\mathrm{n}} x_{\mathrm{p}} \tag{2}$$

In Eq. (2), F_{N} represents the normal component of the force, or any other load acting on the contact, perpendicular to the contact surface. k_{n} refers to the normal stiffness constant, and x_{p} represents the penetration of one surface into another (see Fig. 2) [12].

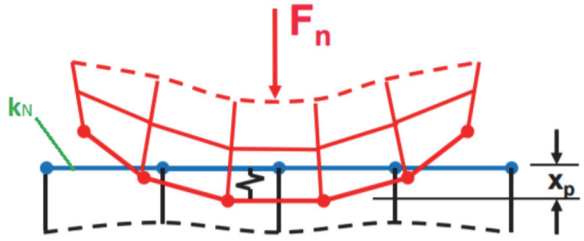

Figure 2 Display of variables in the "Penalty Method" formulation [12]

As already mentioned, a more advanced version of the "Penalty Method" formulation is the "Augmented Lagrange" formulation, where there is an additional variable called Lagrange multiplier λ [12]:

$$F_{\mathrm{N}} = k_{\mathrm{n}} x_{\mathrm{p}} + \lambda \tag{3}$$

The role of the Lagrange multiplier is to control the penetration that occurs during the interaction of two bodies. Due to the properties of the Lagrange multiplier, the "Augmented Lagrange" formulation is not so sensitive to the normal stiffness constant k_{n}. The Lagrange multiplier can be used to manually adjust the stiffness, which directly affects the achievement of convergence or reduction of penetration. The higher the value of the stiffness factor, the less penetration there will be and vice versa [12].

In order to correctly define the contact in the numerical analysis, the surfaces that are in contact must be correctly selected, i.e. the surface that will represent the "Contact" and the surface that will represent the "Target". Fig. 3 shows the selected surfaces for the case of a shrink fit of a disk and a shaft. The outer surface of the shaft was chosen as "Target", and the inner surface of the conical disc was chosen as "Contact", for the reason that the contact surface of the shaft is larger than the contact surface of the conical disc [19].

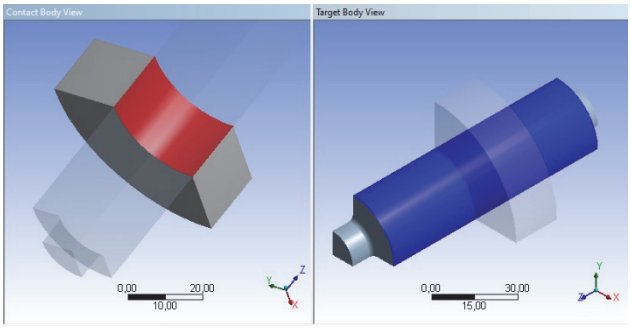

Figure 3 Display of selected "Contact" and "Target" contact surfaces [12]

In numerical analysis, there are two basic contact behaviors, Symmetric and Asymmetric. Correct selection of contact behavior directly affects the accuracy of numerical analysis solutions [19].

During the analysis of the shrink fit, the behavior of the contact is defined as Asymmetric. In the case of Asymmetric contact behavior, the penetration of the "Contact" surface into the "Target" surface is disabled, but the penetration of the "Target" surface into the "Contact" surface is enabled. The values of the results of the contact pressures in the case of asymmetric behavior will be displayed only on the "Contact" side of the surface (see Fig. 4) [19].

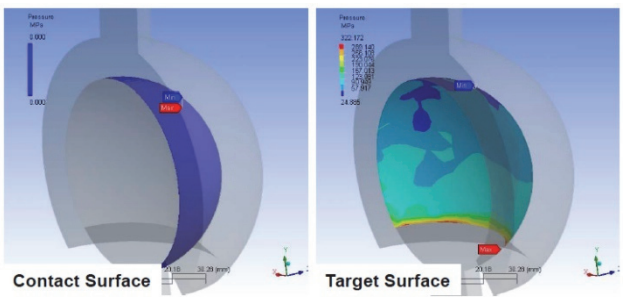

Figure 4 Distribution of contact pressures in case of Asymmetric contact behavior [19]

Also, in the case of Asymmetric behavior, the detection of the contact of nodes that penetrate from one surface to another is performed via integration nodes (e.g. the Gauss method) (see Fig. 5). In this case it is necessary to take steps to reduce this penetration (a denser mesh of finite elements, greater stiffness of the contact surface, ...), which directly affects the accuracy of the numerical analysis results.

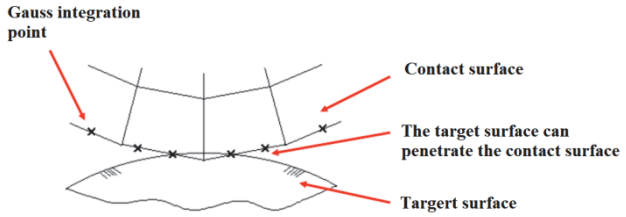

Figure 5 Gauss detection method [12]

2.1 Numerical Model

The model of the conical disc and rotor shaft of the steam turbine is shown in Fig. 6. As inertial forces caused by the masses of the elements in the shrink fit occur during rotation, it is necessary to take into account the mass of all the elements that make up the assembly of the shrink fit. In addition to the conical disc and the shaft, important factors in the shrink fit are also the rotor blades. Due to computer and hardware limitations, a blade model was not added to the disk model, but using the "Distributed Mass" command in Ansys, the mass of the rotor blades was defined on the outer rim of the conical disc [11]. Fig. 6 also shows the definition of the rotor speed of the assembly around the axial *z* axis.

The conical disc-shaft shrink fit transfers the torque from the rotor blades to the turbine shaft. In addition to the shrink fit, the transmission of torque is also ensured by two keys placed diametrically opposite each other. In this analysis, the shrink fit without these two keys was considered.

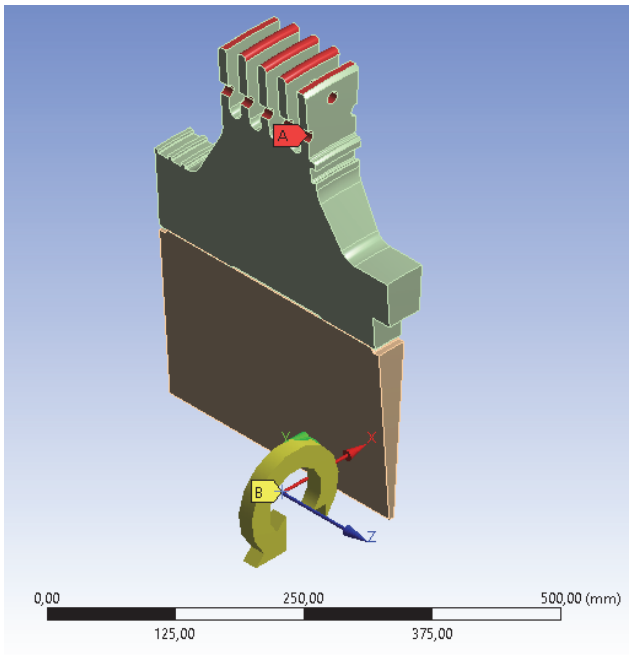

Figure 6 Shrink fit model of the conical disc and the shaft [11]

After defining the model, the next step was to generate the mesh of finite elements. The finite elements used in the numerical analysis are tetrahedral elements of the second order.The global size of the elements is 8 mm, while in the contact area the elements are reduced to 2,5 mm, and 1 mm for places of geometric discontinuities, in order to obtain more accurate stress results (see Fig. 7).

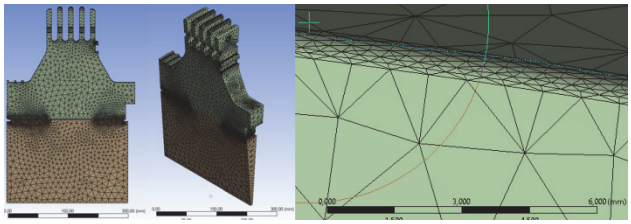

Figure 7 Meshed model of shrink fit [11]

During the numerical analysis, the property of cyclic symmetry of the disk and the shaft was used in order to reduce the load on the computer capacities, and to achieve a faster and simpler calculation.The interference in the shrink fit is geometrically modeled in order to make the results of the numerical analysis more reliable. When using the Cyclic Region option, it is necessary to define the Low Boundary and High Boundary in order for the numerical calculation to be performed correctly see (Fig. 8).

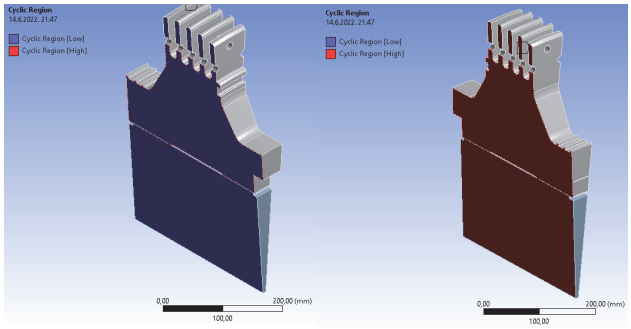

Figure 8 Cyclic Region option [11]

The nominal measurement of the bore diameter of the conical disc is $505^{+0,07}_{0}$ mm, while the nominal measurement of the shaft diameter is $505^{+0,6}_{+0,54}$ mm.

During the analysis of the disc-shaft shrink fit, special attention was paid to the operating rotor speed (3000 rpm), and the speed at which the turbine trips due to overspeed protection (3300 rpm). The rotor speed at which the disc-shaft interference disappears is determined using the calculated value of the maximum contact pressure for different rotor speed. When the maximum contact pressure takes on the value 0 at a certain rotor speed, the disc is released from the shaft, i.e. the shrink fit no longer exists.

2.2 Analysis of the Shrink Fit with the Minimal Interference Value

The minimal interference value $P_{\min}$ is obtained by pairing the sleeve with the smallest diameter and the bore with the largest diameter. The smallest diameter of the shaft according to the given tolerances is 505,54 mm, while the largest diameter of the disc bore is 505,07 mm, and the expression for the minimal value of the interference is [20]:

$$P_{\min} = 2\delta = ei - ES \quad (4)$$

where *ei* is lower limit deviation of the shaft sleeve; *ES* is upper limit deviation of the hub bore. The calculated value of $P_{\min}$ is 0,47 mm.

Before conducting the analysis, the rotor speed range for which the behavior of the shrink fit will be analyzed is defined. Fig. 9 presents a graphical and tabular representation of rotor speeds by steps.

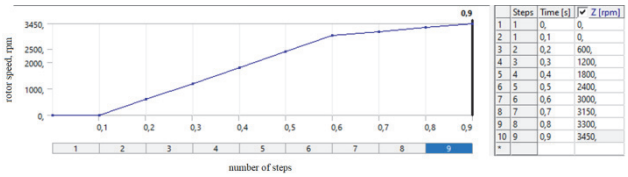

Figure 9 Graphical and tabular representation of rotor speed by steps for the minimal interference value [11]

The performed analysis shows that as the speed increases, the contact pressure of the shrink fit decreases as expected. Fig. 10 shows the dependence of the maximum contact pressure on the rotor speed. It can be seen that the contact pressure reaches a value of zero at 3300 rpm. This is the rotor speed at which the interference between the disc and the rotor shaft is lost. At operating speed of the rotor (3000 rpm), the maximum value of the contact pressure is 47,27 MPa, which ensures the normal transfer of torque. The speed at which the shaft-disc connection is lost is the speed at which the turbine trips due to overspeed protection. This means that in the range of possible rotor speeds there is no risk of vibration due to the looseness of the disc-shaft connection.

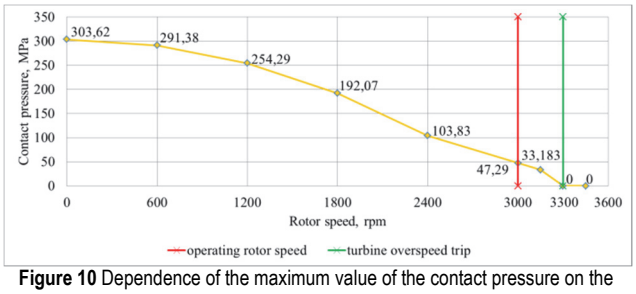

Figure 10 Dependence of the maximum value of the contact pressure on the rotor speed for the minimal interference value [11]

The rotor speed at which disc-shaft interference is lost can also be determined using the disc-to-shaft gap value. Fig. 11 shows that the gap is zero until 3300 rpm. Above this speed, the gap starts to increase in absolute value. This means that at speed 3300 rpm the disc-shaft interference is lost. This speed value matches the rotor speed obtained using the contact pressure analysis.

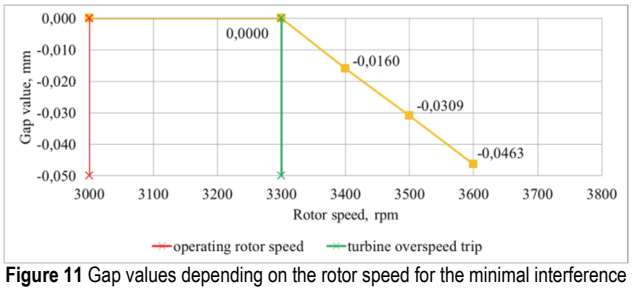

Figure 11 Gap values depending on the rotor speed for the minimal interference value [11]

A series of graphic representations of contact pressure distribution of the shrink fit for different rotor speeds is given in Fig. 12. It can be seen that the disc begins to separate from the shaft first at its inner edges of both contact surfaces. As the rotor speed increases, the separation of the disc from the shaft propagates from the inner to the outer edges of the contact surfaces. Also, complete separation of the disc from the shaft first occurs on a narrower contact surface, and then, at 3300 rpm, on a wider one. This is the speed at which the disc-shaft shrink fit disappeared.

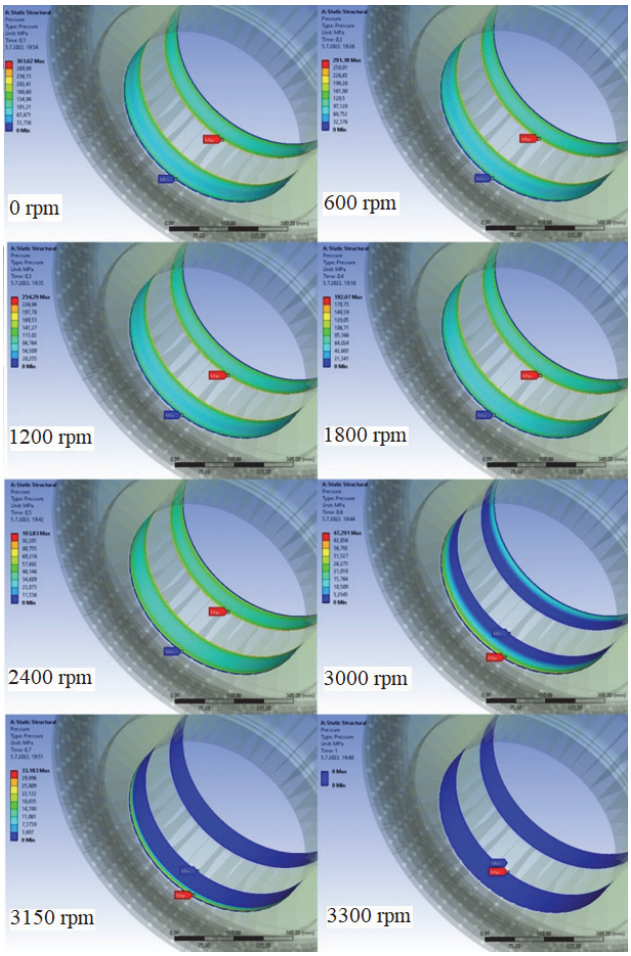

Figure 12 Series of graphic displays of the shrink fit contact pressure distribution at different rotor speeds for the minimal interference value [11]

2.3 Analysis of the Shrink Fit with the Maximum Interference Value

The maximum interference value $P_{\max}$ is obtained by pairing the sleeve with the largest diameter and the bore with the smallest diameter. The largest diameter of the shaft according to the given tolerances is 505,6 mm, while the smallest diameter of the disc bore is 505,0 mm, and the formula for the maximum value of the interference is [20]:

$$P_{\max} = 2\delta = es \quad (5)$$

where *es* is upper limit deviation of the shaft sleeve. The calculated value of $P_{\max}$ is 0,6 mm.

Fig. 13 presents a graphical and tabular representation of the rotor speeds by steps during which the behavior of

the shrink fit will be analyzed at the maximum interference value.

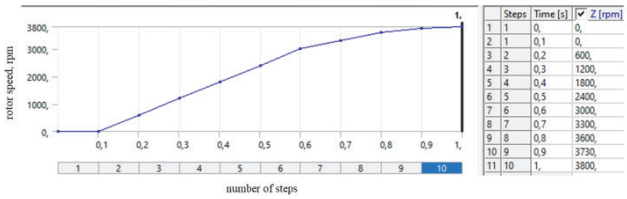

Figure 13 Graphical and tabular presentation of rotor speed by steps for the maximum interference value [11]

Fig. 14 shows the change in the maximum contact pressure of the shrink fit as a function of the rotor speed. The contact pressure reaches the value zero at 3730 rpm. This rotor speed represents the speed at which the interference between the disc and the rotor shaft is lost. Also, the contact pressure values for different rotor speeds can be read from the diagram. At the operating speed (3000 rpm), the maximum value of the contact pressure of the shrink fit is 93.265 MPa, while at the speed at which the turbine trips (3300 rpm), the maximum value of the contact pressure is 69,736 MPa. It means that the torque can be transmitted smoothly. Also, there is no risk of vibration due to the looseness of the disc-shaft connection in the range of possible rotor speeds.

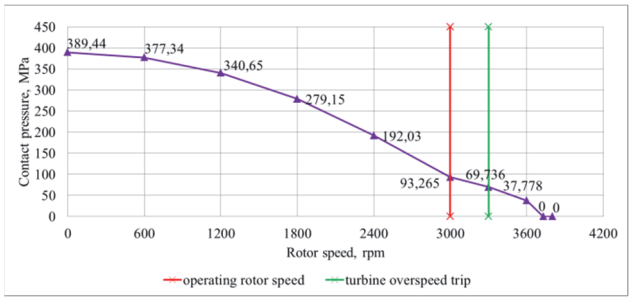

Figure 14 Dependence of the maximum value of the contact pressure on the rotor speed for the maximum interference value [11]

In Fig. 15, it is visible that the gap between disc and shaft is zero up to a speed of 3730 rpm. Above this speed, the gap starts to increase in absolute value. This means that at speed 3730 rpm the disc-shaft interference is lost. Identical speed was obtained using contact pressure analysis.

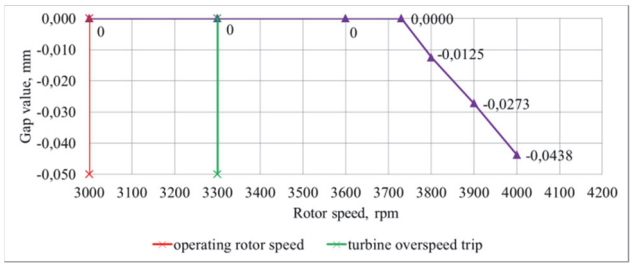

Figure 15 Gap values depending on the rotor speed for the maximum interference value [11]

Fig. 16 shows a series of graphic representations of contact pressure distribution of the shrink fit for different rotor speeds. Identical conclusions can be drawn as in the case of shrink fit with minimal interference.

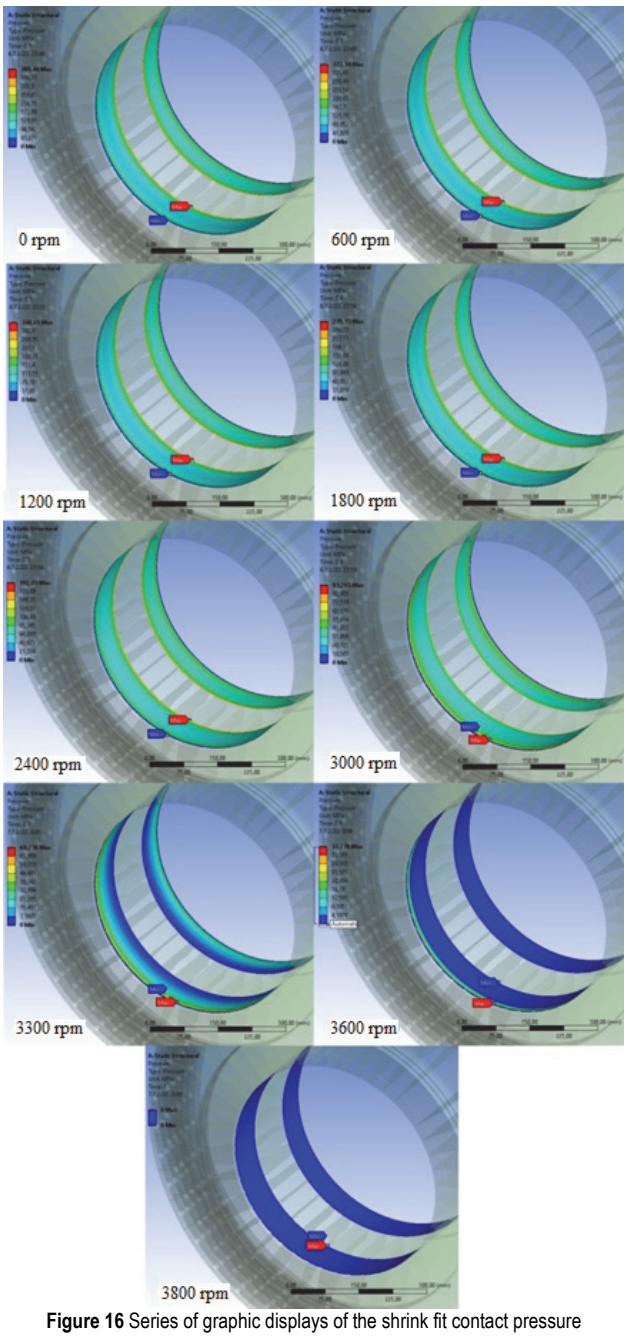

Figure 16 Series of graphic displays of the shrink fit contact pressure distribution at different rotor speeds for the maximum interference value [11]

2.4 Analysis of the Shrink Fit with the Mean Interference Value

The actual value of the interference ranges between P_{max} and P_{min}, in absolute terms. The mean interference value will be determined from the arithmetic mean of the tolerances for the bore of the conical disc and the outer diameter of the shaft.

The arithmetic mean of the shaft diameter tolerance is 505,57 mm, while the arithmetic mean of the conical disc bore tolerance is 505,035 mm. The value of the interference in this case is as follows [20]:

$$P_{av} = 2\delta = e_{av} - E_{av} \tag{6}$$

where e_{av} is mean deviation of the shaft sleeve; E_{av} is mean deviation of the hub bore. The calculated value of P_{av} is 0,535 mm.

Fig. 17 presents a graphical and tabular representation of the rotor speeds by steps during which the behavior of the shrink fit at the mean interference value will be analyzed.

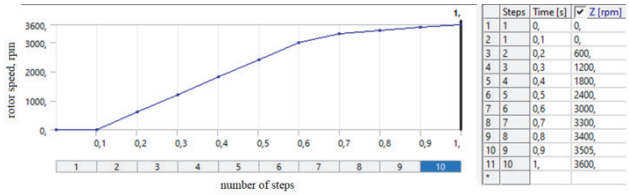

Figure 17 Graphical and tabular presentation of rotor speed by steps for the mean interference value [11]

Fig. 18 shows the dependence of the maximum contact pressure on the rotor speed. The contact pressure reaches the value zero at 3505 rpm. This rotor speed is the speed at which the interference between the disc and the rotor shaft is lost. At operating speed of the rotor (3000 rpm), the maximum value of the contact pressure is 70,507 MPa, which ensures the normal transfer of torque. At the speed at which the turbine trips (3300 rpm), the maximum value of the contact pressure is 44,168 MPa. It means that the torque can be transmitted smoothly and there is no risk of vibration due to the looseness of the disc-shaft connection in the range of possible rotor speeds.

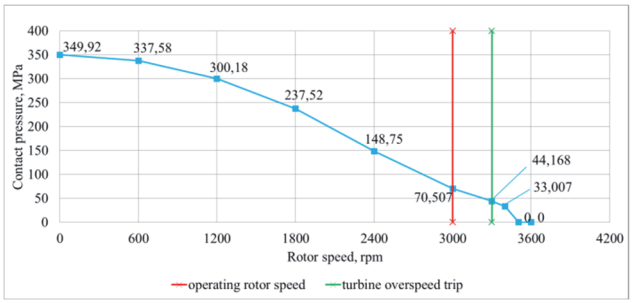

Figure 18 Dependence of the maximum value of the contact pressure on the rotor speed for the mean interference value [11]

Fig. 19 shows that the gap is zero until the speed of 3505 rpm, after which the gap starts to increase in absolute value. This means that at speed 3505 rpm the disc-shaft interference is lost. The same speed value is obtained using the contact pressure analysis.

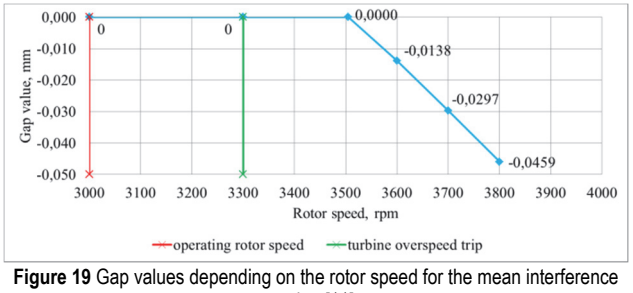

Figure 19 Gap values depending on the rotor speed for the mean interference value [11]

A series of graphic representations of contact pressure distribution of the shrink fit for different rotor speeds is given in Fig. 20. Identical conclusions can be drawn as in the case of shrink fit with minimal and maximum interference.

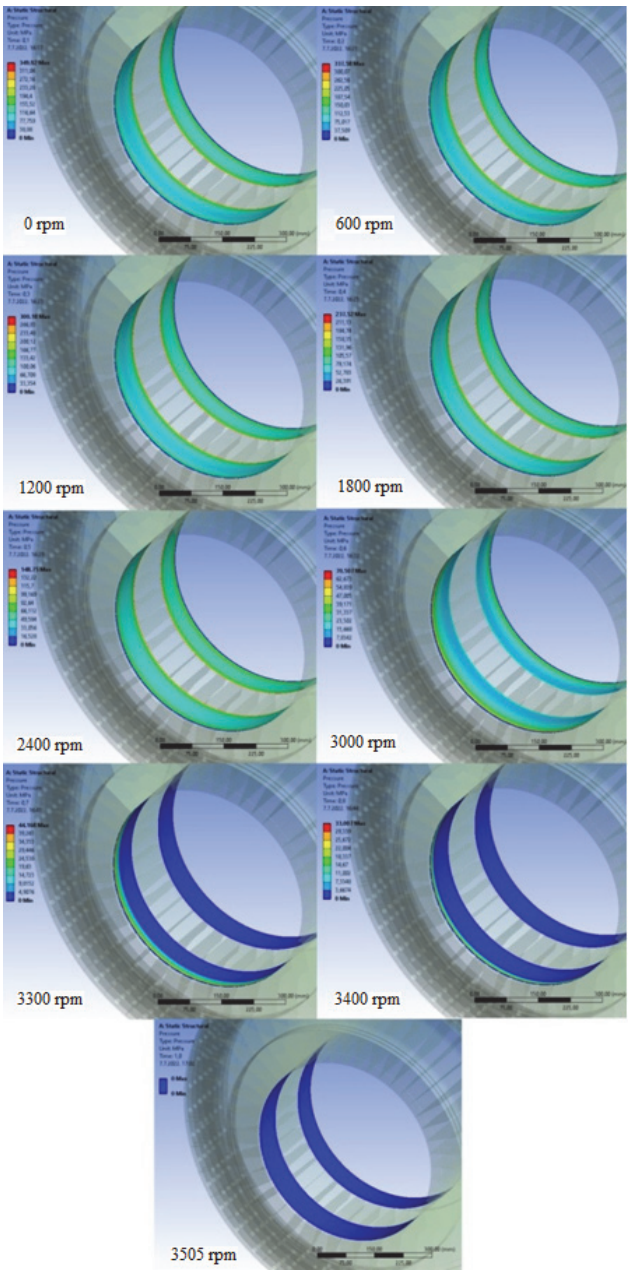

Figure 20 Series of graphic displays of the shrink fit contact pressure distribution at different rotor speeds for the mean interference value [11]

3 RESULTS AND DISCUSSION

Numerical analysis of the shrink fit of the conical disc-shaft was carried out for three different values of interference obtained using the design tolerances of the disk bore and the shaft sleeve: minimum, maximum and mean value. The goal of the analysis was, for each interference value considered, to determine the rotor speed at which the shrink fit is lost. The criterion for loss of shrink fit was the zero value of the contact pressure in the disc-shaft connection. Fig. 21 shows a comparison of the variation of the maximum contact pressure value depending on the rotor speed for different interference values.

Useful information can be obtained from this Fig. 21.

The maximum contact pressure values at rotor operating speed (3000 rpm) are as follows:

- for minimal interference: 47,29 Mpa
- for mean interference: 70,51 MPa

- for maximum interference: 93,27 Mpa.

Maximum contact pressure values at the speed at which the turbine trips due to overspeed protection (3300 rpm) are:

- for minimal interference: 0 MPa
- for mean interference: 44,17 MPa
- for maximum interference: 69,74 MPa.

Rotor speeds at which shrink fit is lost are:

- for minimal interference: 3300 rpm
- for mean interference: 3505 rpm
- for maximum interference: 3730 rpm.

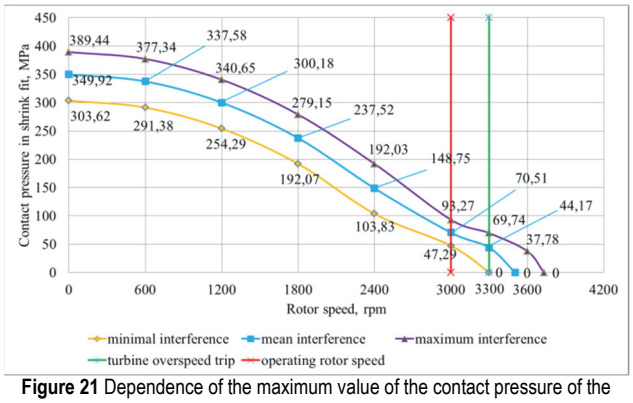

Figure 21 Dependence of the maximum value of the contact pressure of the shrink fit on the rotor speed for different interference values [11]

A comparison of the change in the gap in the shrink fit of the conical disk and the shaft depending on the rotor speed for different interference values is shown in Fig. 22. It is clearly visible that the rotor speed at which the gap begins to appear for the considered interference values coincides with the values obtained from the contact pressure analysis.

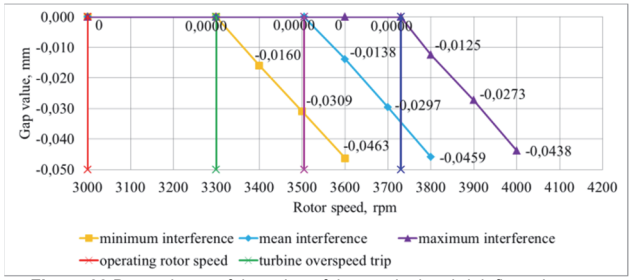

Figure 22 Dependence of the value of the gap in the shrink fit on the rotor speed for different values of the interference [11]

The analysis of the results shows that the shrink fit for all considered disc-shaft interference values will be stable and safe at the operating speed of the rotor (3000 rpm). The analysis of the results shows that the shrink fit for all considered disc-shaft interference values will be stable and safe at the operating speed of the rotor (3000 rpm). However, for the minimum value of the interference and at the turbine trip speed (3300 rpm) the shrink fit is lost. For this reason, and to achieve additional safety, the minimal value of interference in the shrink fit should be avoided, and an optimal interference should be achieved.

An optimal interference must meet two conditions, namely that it must exist at the operating speed to enable the transfer of torque from the blades, but it should not have an excessive value that would cause stress concentrations that would cause local material flow, i.e. plastics deformation. As already stated earlier, the actual interference value in the shrink fit ranges between P_{max} and P_{min}, in absolute terms. The highest frequency of use is the mean interference values, while the frequency of use of the limit values is significantly lower. Achieving a mean interference value ensures a stable shrink fit in the entire range of operating speeds up to the trip speed. On the other hand, the maximum stresses in shrink fit are theoretically lower than the stresses that would appear in case of maximum interference value.

4 CONCLUSIONS

The main goal of this work was the analysis of the conical disk-shaft shrink fit and the determination of the rotor speed at which this fit is lost. This speed was found according to two criteria: the contact pressure on the disc-shaft contact surfaces and the gap between the disc and the shaft. Three design values of disc-shaft joint interference were considered: minimum, maximum and mean. The results obtained by both applied criteria are consistent. The rotor speed at which the shrink fit is lost is the lowest for minimum interference (3300 rpm) and the highest for maximum interference (3730 rpm), which was expected. For mean interference this speed is 3505 rpm. All speeds obtained are higher than the constant operating speed (3000 rpm), which ensures smooth torque transfer for all considered interferences. For minimal interference, the speed at which the shrink fit is lost corresponds to the turbine trip speed due to overspeed protection (3300 rpm). This should not cause a problem, as this is not the speed at which the turbine operates. However, usually in practice the mean value of the interference is realized, which increases the speed at which the shrink fit is lost to a higher value. In the end, it can be concluded that the considered shrink fit ensures the transfer of torque in the range of speeds up to the operating speed and that the operation of the turbine is safe from this point of view.

5 REFERENCES

[1] Collins, J. A., Busby, H., & Staab, G. (2010). *Mechanical design of machine elements and machines - A failure prevention perspective*. Wiley Publication.

[2] Shigley, J. E. & Mischke, C. R. (1996). *Standard Handbook of Machine Design*. McGraw-Hill: New York.

[3] Yang, G. M., Coquille, J. C., Fontaine, J. F., & Lambertin, M. (2002). Contact pressure between two rough surfaces of a cylindrical fit. *Journal of Materials Processing Technology*, *123*(3), 490-497. https://doi.org/10.1016/S0924-0136(02)00139-5

[4] Wang, X., Lou, Z., Wang, X., & Xu, C. (2017). A new analytical method for press-fit curve prediction of interference fitting parts. *Journal of Materials Processing Technology*, 250, 16-24. https://doi.org/10.1016/j.jmatprotec.2017.06.022

[5] Cui, Y., Zhang, L., Zhang, C., Li, R., & Li, F. (2021). Stress analysis of shrink fitting process of ultra-thin reactor coolant pump rotor-can. *Annals of Nuclear Energy*, *162*, 108492. https://doi.org/10.1016/j.anucene.2021.108492

[6] Lewis, R., Marshall, M. B., & Dwyer-Joyce, R. S. (2005). Measurement of interface pressure in interference fits. *Journal of Mechanical Engineering Science*, *219*(2), 127-139. https://doi.org/10.1243/095440605X8432

[7] Madej. J. & Sliwka, M. (2021). Analysis of interference-fit joints. *Applied Sciences*, *11*(23), 11428. https://doi.org/10.3390/app112311428

[8] Gopalakrishnan, V., Batrani, M., Mohan, J., Bhatt, N. C., & Verma, M., K., (2017). Design of Shrink Fit for Low Temperature Rotating Turbine Components. *International Journal of Engineering Research & Technology*, *6*(4), 1-4. https://doi.org/10.17577/IJERTV6IS040028
[9] Tan, S., Chen, G., Wang, W., & Chen, H. (2013). Stress Analysis on Complex Shrunk-on Rotor of Steam Turbines, *Journal of Chinese Society of Power Engineering*, *33*(8), 581-585.
[10] Ansys Inc.: ANSYS 17.2
[11] Travica, D. (2022). *Static and dynamic analysis of a disk of an action steam turbine rotor*. Graduate Thesis, Mechanical Engineering Faculty in Slavonski Brod (in Croatian).
[12] Gai, S., Zhao, J., Lin, F., Li, A., & Liu, S. (2023). Optimization of Forged 42CrMo4 Steel Piston Pin Hole Profile Using Finite Element Method. *Tehnicki vjesnik-Technical Gazette*, *30*(1), 80-86. https://doi.org/10.17559/TV-20220330131907
[13] Ozkal, F. M., Cakir, F., & Arkun, A. K. (2016). Finite element method for optimum design selection of carport structures under multiple load cases. *Advances in Production Engineering & Management*, *11*(4), 287-298. https://doi.org/10.14743/apem2016.4.227
[14] Lamprecht, M. & Leonhartsberger, M. (2021). Tool Stiffness Calculation in Roll Forming. *International Journal of Simulation Modelling*, *20*(1), 40-51. https://doi.org/10.2507/IJSIMM20-1-539
[15] Kalay, O.C., Karaman, H., Karpat, F., Doğan, O., Yüce, C., Karpat, E., Khandaker, M. et al. (2021). A Comparative 3D Finite Element Computational Study of Stress Distribution and Stress Transfer in Small-Diameter Conical Dental Implants. *Tehnicki vjesnik-Technical Gazette*, *28*(6), 2045-2054. https://doi.org/10.17559/TV-20200518180158
[16] Stefanovska, E. & Pepelnjak, T. (2022). Development of a flexible tooling system for sheet metal bending. *Advances in Production Engineering & Management*, *17*(3), 311-325. https://doi.org/10.14743/apem2022.2.429
[17] Li, X. J., Wang, D., & Saeed, T. (2022). Multi-Scale Numerical Approach to the Polymer Filling Process in the Weld Line Region. *Facta Universitatis-Series Mechanical Engineering*, *20*(2), 363-380. https://doi.org/10.22190/FUME220131021L
[18] Maksimovic, M., Maksimovic, K., Stamenkovic, D., & Vasovic Maksimovic, I. (2021). Initial Fatigue Life Estimation of Welded Structural Components. *Tehnicki vjesnik-Technical Gazette*, *28*(4), 1099-1104. https://doi.org/10.17559/TV-20200414015501
[19] ANSYS, Inc. (2009). Introduction to Contact: Workbench - Mechanical Structural Nonlinearities Retrieved from https://docplayer.net/143443957-Lecture-3-introduction-to-contact-16-0-release-ansys-mechanical-introduction-to-structural-nonlinearities-ansys-inc.html
[20] Opalić, M. & Kljajin, M. (2010). *Engineering graphics, University textbook*. SlavonskiBrod.

Contact information:

Marko KATINIĆ, PhD, Associate Professor
(Corresponding author)
Mechanical Engineering Faculty, University of Slavonski Brod
Trg I. B. Mažuranić 2, 35000 Slavonski Brod, Croatia
E-mail: mkatinic@unisb.hr

Domagoj TRAVICA, Mag. Ing. Mech.
Mechanical Engineering Faculty, University of Slavonski Brod
Trg I. B. Mažuranić 2, 35000 Slavonski Brod, Croatia
E-mail: dtravica@unisb.hr

Pejo KONJATIĆ, PhD, Full Professor
Mechanical Engineering Faculty, University of Slavonski Brod
Trg I. B. Mažuranić 2, 35000 Slavonski Brod, Croatia
E-mail: pkonjatic@unisb.hr

Mladen BOŠNJAKOVIĆ, PhD, Assistant Professor
Technical Department, University of Slavonski Brod
Trg I. B. Mažuranić 2, 35000 Slavonski Brod, Croatia
E-mail: mbosnjakovic@unisb.hr